Constitutive modelling of hyperelastic rubber-like materials

Z. Guo and L. J. Sluys

Delft University of Technology, Delft, The Netherlands

The simulation of rubber-like material behaviour by means of the finite element method has been described in this study. Proper material models were selected for the numerical description of static hyper-elasticity. The combinations of a continuum damage mechanics concept and a pseudo-elastic concept with Gao's elastic law were used to simulate the ideal Mullins effect. Furthermore, a specific model describing the Mullins effect with permanent deformation was proposed. Another focus of this study was the verification of numerical constitutive models by means of experimental evidence, which is essential for the proper description of the behaviour of rubber-like materials in engineering applications.

Key words: Rubber-like material, constitutive modelling, Mullins effect, continuum damage mechanics, pseudo-elastic model, finite element method

1   Introduction

Rubber-like materials exhibit a highly nonlinear behaviour characterized by hyperelastic deformability and incompressibility or near-incompressibility. Normally, the maximum extensibility of rubber could reach values varying from 500% to 1000% and the typical stress-strain curve in tension is markedly nonlinear so that Hooke's law can not be used and it is not possible to assign a definite value to the Young's modulus except in the region of small strains, where the Young's modulus is of the order of 1MPa. In contrast, the Young's modulus for typical hard solids is in the region 10^4-10^6 MPa and the maximum elastic extensibility of hard solids seldom exceeds 1%. Rubber-like materials are effectively incompressible in most cases. However, all real materials are compressible to a certain degree even if the bulk modulus is several orders of magnitude larger than the shear modulus.

Many attempts have been made to develop a theoretical stress-strain relation that fits experimental results for hyperelastic materials. There are two different phenomenological approaches to the study of rubber elasticity. Firstly, a theory treats the problem from the

viewpoint of continuum mechanics and, secondly, a statistical or kinetic theory attempts to derive elastic properties from some idealized model of the structure of vulcanised rubber. The representative works can be found in the literature Mooney [1940], Treloar [1944], Rivlin [1948a, b, 1949], Yeoh [1993], Gent [1996] and Ogden [1972a, b]. Besides these purely phenomenological models, a micro-mechanically based idealized network concept has also been proposed. Typical models are proposed by Khun and Grun [1942], James and Guth [1943], Wang and Guth [1952], Treloar [1946], Flory and Rehner [1943], Wu and Van der Giessen [1993], Charlton and Yang [1994], Boyce [1996], Boyce and Arruda [2000] , Miehe et al. [2004] and Guo [2006]. Theoretical analysis and engineering application require a constitutive law to be expressed as simple as possible, especially, when we consider complicated singular problems (Knowles and Sternberg, 1973; Mooney, 1940) and stress-softening. However, simplicity often violates rationality. To reflect material behaviour under such situations and to come up with a reasonable and applicable elastic law is still an important issue in nonlinear elasticity theory.

Moreover, when a rubber specimen is subjected to cyclic loading the stress-softening phenomenon has been observed. Bouasse and Carriere [1903] first found this phenomenon in a test for a rubber vulcanizate. As a consequence of a more extensive experimental investigation by Mullins [1947], the stress softening effect is now widely known as the Mullins effect. Many researchers have studied this effect by means of both molecular-based and phenomenological-based models. More details can be found in references of Mullins [1947], Mullins and Tobin [1957], Harwood et al [1967], Johnson & Beatty [1993], Beatty and Krishnaswamy [2000], Qi and Boyce [2004], Gurtin and Francis [1981], Simo [1987], Govindjee & Simo [1992a, b], Miehe [1995], Chagnon et al. [2004] Ogden and Roxburgh [1999] and Boyce and Arruda [2000]. Among these proposed methods, the continuum damage mechanics (CDM) approach and the pseudo-elastic model are often employed to describe Mullins effect. The basic mechanisms of the two models are completely different, so that comparison of the two models showing the advantages and limitations will be beneficial to engineering applications.

Another phenomenon for carbon-filled rubber is that after loading and subsequent unloading rubber specimens, in general, do not return to their initial state, but exhibit a residual deformation. The permanent deformation combined with stress-softening effects results in complex mechanical behaviour and modelling is still at an early stage. Lion [1996], Septanika [1998], Miehe and Keck [2000], Drozdov and Dorfmann [2001] and Besdo and Ihlemann [2003] made their contributions to this field. Recently, Dorfmann and Ogden [2004] used pseudo-elasticity to capture Mullins effect and residual strain with the

inclusion of two variables in the energy function. But, this model cannot describe evolution of rubber softening and permanent deformation and has too many adjustable parameters, which can, to some degree, only be determined arbitrarily [Zhong 2005].

The present work was motivated by the need for an appropriate material model, to be used for hyperelastic materials, which contains a small number of parameters and is able to describe the material response for different deformation modes under reasonable high deformation levels. The second purpose of this study is concerned with constitutive models, which incorporate the stress-softening phenomena. The CDM concept and a pseudo-elastic model combined with Gao's elastic law are proposed to describe ideal Mullins effect, respectively. Finally, a specific constitutive model to capture the Mullins effect and its corresponding permanent deformation is proposed.

2   Mullins effect

Fig. 1 depicts the curve of the stress against stretch λ for the stress-softening or Mullins effect in a simple tension test. Under cyclic loading conditions, the load required to produce a given stretch during the second loading cycle (along branch aBb' in Fig. 1) is smaller than the load required to produce the same stretch during the primary loading cycle (abb').

Experimental evidence by Mullins (1947) and Mullins and Tobin (1957) show that a model for filled rubber vulcanizates excluding the permanent deformations is an ideal representation of the stress softening as shown in Fig. 1a. The stress-stretch response upon initial loading of a material, which has experienced no previous deformation, is defined as the virgin response and the corresponding stress-stretch path is called the virgin material curve or primary loading path (path b in Fig. 1a). The stress-stretch response upon unloading of a material is called the stress-softening response and the corresponding stress-stretch path is called the stress-softening material curve or unloading or secondary loading path. If the stretch is increased beyond historic maximum stretch (e.g. $\lambda_{b'}$), the material response starting at $\lambda_{b'}$ follows the virgin curve as if unloading has not taken place. So, for an ideal representation of stress softening, the curve bb'cc'd in Fig. 1a is defined as the virgin material curve or primary loading path.

Unlike the above-introduced ideal stress-softening phenomenon, in fact, a typical stress-stretch response of a rubber material under cyclic loading with a constant maximum stretch-amplitude is illustrated in Fig. 1b. In the first cycle, the loading-unloading path is as shown by the solid line. In the next cycles, the loading-unloading paths (dotted line) will

approximately follow the unloading path of the first cycle, but will not exactly coincide with it. The loading-unloading path of the stress-stretch response becomes quasi-consistent for the k-th cycle where $k \geq k_m$. A typical value of k_m for rubber lies between 5 and 10 (Lion 1996, Septanika 1998, Ogden 2004). Many experimental investigations demonstrate that stress softening in successive loading cycles is most significant during the first and second cycle, so the ideal stress-softening model as described by means of Fig. 1a can represent the main characteristics without loss of generality.

Fig. 2 illustrates the more complicated case of the stress softening phenomenon combined with permanent deformation. Different from the ideal Mullins effect, after loading and subsequent unloading, the rubber specimens do not return to their initial state (A), but exhibit residual deformation (AA′); If the stretch is reincreased beyond historic maximum stretch (e.g. λ_B), the material response (after λ_B) will not follow the virgin curve (BE), but follow the curve (CD) and finally return to the virgin curve at D.

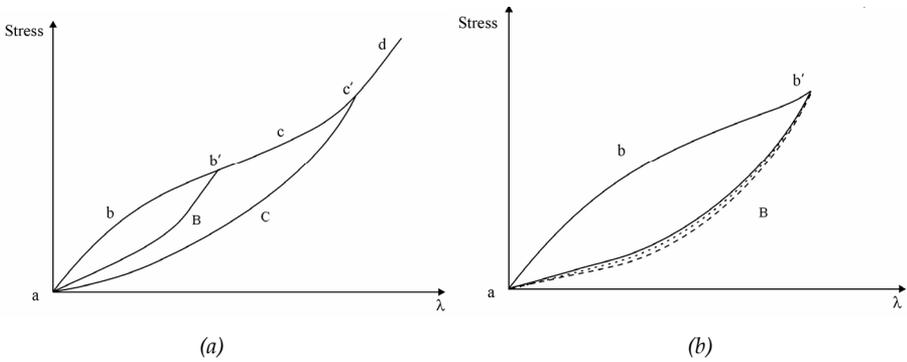(a)   (b)

Figure 1 A. schematic uniaxial stress-stretch response (a) for an ideal stress softening material; (b) for the stress softening under repetitive loading with a constant maximum stretch-amplitude
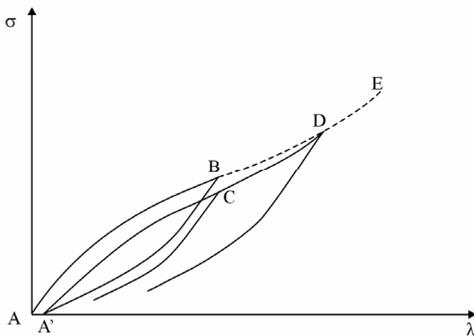

Figure 2 A. schematic uniaxial stress-stretch response of a stress softening material with residual strain

112

3   Constitutive models

3.1   New constitutive model for rubber-like materials

Gao proposed a strain energy function that separately considers the resistance of materials to tension and compression. Accordingly, a strain energy formulae that only contains two terms was given by Gao [1997]

$$W = a\left(I_1^n + I_{-1}^n \right) \tag{1}$$

where a and n are model parameters. Both I_1 and I_{-1} are strain invariants. The second Piola-Kirchhoff stress $\boldsymbol{\tau}$ becomes

$$\boldsymbol{\tau} = 2\frac{\partial W}{\partial \mathbf{C}} = 2an\left(I_1^{n-1}\mathbf{I} - I_{-1}^{n-1}\mathbf{C}^{-2} \right) \tag{2}$$

Where $\mathbf{C}$ is right Cauchy-Green strain tensor. The second Piola-Kirchhoff stress tensor is a useful stress measure in numerical programmes. For engineering purposes the Cauchy stress tensor $\boldsymbol{\sigma}$ is more appropriate. Both stress measures are related via

$$\boldsymbol{\sigma} = J^{-1}\mathbf{F}\cdot\boldsymbol{\tau}\cdot\mathbf{F}^T \tag{3}$$

where J is the Jacobian of the transformation and $\mathbf{F}$ is the deformation gradient tensor for an undamaged elastic material. Let λ_i denote the values of principal strain,

$$\begin{aligned}
I_1 &= \lambda_1^2 + \lambda_2^2 + \lambda_3^2 \\
I_{-1} &= \lambda_1^{-2} + \lambda_2^{-2} + \lambda_3^{-2} \\
J &= \lambda_1\lambda_2\lambda_3
\end{aligned} \tag{4}$$

The stress $\boldsymbol{\tau}$ and the incremental stress-strain relation $\mathbf{D}$, which can be derived from Eq. (2), are basic equations for implementation of the proposed model in finite element software. It is important that the energy function obey the laws of thermodynamics when energy functions are used to relate stress and strain in finite element programs. In other words, energy functions should mathematically require the solid to increase its internal energy when we do work on it. As pointed out by Johnson *et al.* [1994] unstable energy functions can cause great havoc in the nonlinear numerical solution algorithms used in the finite element codes. Stability requires energy functions to obey a certain condition, which is known as Drucker's stability postulate that can be expressed as follows:

$$\sum_i d\sigma_i d\varepsilon_i \geq 0 \tag{5}$$

where $d\sigma_i$ is an increment in the i'th principal Cauchy stress and $d\varepsilon_i$ is an increment in the corresponding strain at any point in the solid. For the case of plane stress, the material is stable when the tangential stiffness matrix $\mathbf{D}$ is positive definite. Johnson et al. [1994]

113

derived Drucker's stability postulate for the form of Rivlin's expansion under the condition of plane stress. Gao's model is a type of polynomial function of invariants, for an incompressible material, Drucker's stability postulate can be expressed as

$$\frac{\partial^2 W}{\partial I_1^2}\frac{\partial^2 W}{\partial I_{-1}^2} - \frac{\partial^2 W}{\partial I_1 \partial I_{-1}} = a^2 n^2 (n-1)^2 I_1^{n-2} I_{-1}^{n-2} - 0 > 0 \tag{6}$$

Generally, $a > 0$ and $1 < n < 3$ [Gao, 1997], so that Gao's model satisfies Drucker's stability postulate. Here, the power n is not necessarily an integer.

3.2 CDM model to represent the ideal Mullins effect

The Mullins effect is due to the rearrangement of the polymer network under deformation when some links between chains, or chains and reinforced particles (e.g. carbon black) are broken [Bueche, 1961, Chagnon at el. 2004]. The process is complex since it involves chain and multi-chain damage, microstructural damage and microvoid formation [Gent 1976, Kramer 1983, Simo 1987]. From the viewpoint of CDM, for an ideal Mullins-type damage evolution, it is assumed that damage accumulation occurs only within the first cycle of a strain controlled loading process. Further strain cycles below maximum effective strain energy do not contribute to this type of damage.

Let us consider an isotropic, homogeneous and incompressible rubber-like material initially characterized by a strain energy function W_0 undergoing isotropic damage. According to CDM theory [Simo 1987, Miehe 1995, Chagnon et al. 2004], a strain energy function W can be expressed in terms of the undamaged (virgin material) W_0.

$$W(\mathbf{F}, d) = (1-d)W_0(\mathbf{F}) \tag{7}$$

where $d \in (0,1)$ is a scalar damage variable which describes an isotropic damage effect characterized by elastic softening of the material and $(1-d)$ is a reduction factor that was suggested by Kachanov [1986] and Lemaitre and Chaboche [1990]. In order to establish the law of state, the Clausius-Duhem inequality for the internal dissipation has been considered [Simo 1987, Miehe 1995].

$$-\dot{W} + \boldsymbol{\tau} : \dot{\mathbf{E}} \geq 0 \tag{8}$$

Where $\dot{\mathbf{E}}$ is the rate of strain tensor, $\boldsymbol{\tau}$ and $\mathbf{E}$ are conjugate pairs of stress and strain tensor, respectively. In this paper $\mathbf{E}$ is the Green-Lagrange strain tensor and $\boldsymbol{\tau}$ is the second Piola-Kirchhoff stress. Substitution of Eq. (7) into Eq. (8) gives

$$-((1-d)\frac{\partial W_0}{\partial \mathbf{E}} : \dot{\mathbf{E}} - W_0 \dot{d}) + \boldsymbol{\tau} : \dot{\mathbf{E}} = \left(\boldsymbol{\tau} - (1-d)\frac{\partial W_0}{\partial \mathbf{E}}\right) : \dot{\mathbf{E}} + W_0 \dot{d} \geq 0 \tag{9}$$

The inequality for every choice of $\dot{\mathbf{E}}$ needs the necessary condition, so, the constitutive hyperelastic equation is achieved

$$\boldsymbol{\tau} = (1-d)\frac{\partial W_0(\mathbf{F})}{\partial \mathbf{E}} = (1-d)\boldsymbol{\tau}_0 \tag{10}$$

where $\boldsymbol{\tau}$ and $\boldsymbol{\tau}_0$ are respective stresses of current and undamaged states. Substituting Eqs. (9) – (10) into Eq. (8), the Clausius-Duhem inequality is reduced to

$$-\frac{\partial W(\mathbf{F},d)}{\partial d}\dot{d} \equiv W_0(\mathbf{F})\dot{d} = f\dot{d} \geq 0 \tag{11}$$

Where f is denoted as the thermodynamic force, which drives damage evolution. It turns out that f is identical to the effective strain energy W_0. Therefore, it is assumed that the Mullins-type damage is governed by the variable

$$\alpha(t) = \underset{s \in [0,t]}{Max} f(s) \tag{12}$$

Where $\alpha(t)$ is the maximum thermodynamic force or effective strain energy, which has been achieved within time interval [0, t]. Thus the damage criterion can be expressed as

$$\phi = f - \alpha(t) = W_0(\mathbf{F}(t)) - \alpha(t) \leq 0 \tag{13}$$

Inequality of Eq. (13) indicates that the current deformation is not maximum in the history and no damage evolves therefore it is in unloading or reloading path. Considering Eq. (13) as an equality, it defines a damage surface by means of strain energy. The mechanical situations in this case can be determined in terms of

$$\phi = 0 \text{ and } \begin{cases} \dot{f} = \boldsymbol{\tau}_0 : \dot{\mathbf{E}} < 0 & \text{in an unloading direction from the damage state} \\ \dot{f} = \boldsymbol{\tau}_0 : \dot{\mathbf{E}} = 0 & \text{in a neutral direction from the damage state} \\ \dot{f} = \boldsymbol{\tau}_0 : \dot{\mathbf{E}} > 0 & \text{in a loading direction from the damage state} \end{cases} \tag{14}$$

Thus, damage evolution can be summarized as

$$\dot{\alpha} = \begin{cases} \dot{f} = \boldsymbol{\tau}_0 : \dot{\mathbf{E}} & \text{if } \phi = f - \alpha = 0 \text{ and } \dot{f} > 0 \\ 0 & \text{otherwise} \end{cases} \tag{15}$$

This equation indicates the discontinuous character of this damage effect and gives the damage criterion based on the strain energy function so that this model is readily applicable to multi-axial states of deformation. Specially, for computational purposes, the maximum energy value may be stored and compared with the current energy state to determine if further damage is being caused. It can be postulated that the scalar damage variable d is a function of α, which on the loading path is W_0. A specific form of the

damage variable function is borrowed from a damage evolution equation, which Miehe [1995] used to simulate a Mullins-type discontinuous damage evolution:

$$d = d_\infty \left(1 - \exp\left(-\frac{\alpha}{\beta} \right) \right) \tag{16}$$

where d_∞ and β are positive model parameters. The combination of CDM model with Gao's model (W_0) is used in numerical implementation.

3.3 Pseudo-elastic model to represent the ideal Mullins effect

An ideal stress-softening response without permanent deformation has the following characteristics: the stress-strain response upon initial loading of a material, which has experienced no previous deformation, follows the primary loading path; the stress-strain response upon unloading or reloading of a material follows an unloading or secondary loading path; furthermore, the stress-strain response upon reloading returns to the primary loading path when the reloading exceeds previous maximum deformation. Apparently, for ideal stress softening, stress and strain are uniquely related in each branch of a specific cyclic process. The material in loading can be treated as one elastic material, and as another elastic material in unloading. Therefore, the terminology of pseudo-elasticity can be used since stress and strain are uniquely related in each branch of a specific cyclic loading process.

Ogden & Roxburgh [1999] have proposed pseudo-elastic model to describe the damage-induced stress-softening effect in rubber-like solids. Unlike the CDM model, the essence of the theory of pseudo-elasticity is that material behaviour in the loading path and in the unloading or reloading paths is described by different strain energy functions. The switch between strain-energy functions is controlled by the incorporation of a damage variable η into the strain energy function, which is then referred to as a pseudo-elastic energy function $W(\mathbf{F}, \eta)$, and η may be either active or inactive. The specific form of $W(\mathbf{F}, \eta)$ used by Ogden & Roxburgh [1999] is given by:

$$W(\mathbf{F}, \eta) = \eta W_0(\mathbf{F}) + \phi(\eta) \tag{17}$$

where the damage variable η varies with the deformation and satisfies $0 < \eta \leq 1$. $W_0(\mathbf{F})$ is the undamaged strain energy function. $\phi(\eta)$ is referred to as a damage function.

When the material is strained monotonically from a virgin state without any unloading no damage occurs and the behaviour may be described by a strain energy function $W_0(\mathbf{F})$. To be consistent with this framework, the damage variable η is set inactive and chosen to be 1 on the primary loading path and the damage function satisfies $\phi(1) = 0$, Eq. (17) reduces to:

116

$$W(\mathbf{F},1) = W_0(\mathbf{F}) \qquad (18)$$

When η is active, it is taken to be dependent on the deformation gradient (the damage evolves with deformation) and we write this dependence in the form

$$\frac{\partial W}{\partial \eta}(\mathbf{F},\eta) = 0 \qquad (19)$$

By substitution of Eq. (17) into Eq. (19), we obtain

$$-\phi'(\eta) = W_0(\mathbf{F}) \qquad (20)$$

in general, the value of η will depend on the values of the deformation attained on the primary loading path, as well as on the specific formulation of $W_0(\mathbf{F})$ and $\phi(\eta)$ used. Since $\eta{=}1$ at any point on primary loading path from which unloading is initiated, W_m is defined.

$$-\phi'(1) = W_0(\mathbf{F}_\mathrm{m}) = W_\mathrm{m} \qquad (21)$$

In accordance with the properties of $W_0(\mathbf{F})$, W_m increases along the primary loading path. For the purpose of implementation, the damage criterion can be expressed as

$$W \begin{cases} \geq W_\mathrm{m} & W = W_0 = W_\mathrm{m} = \underset{s \in [0,t]}{Max}\left(W(s)\right) & \text{loading} \\ < W_\mathrm{m} & W = \eta W_0 + \phi & \text{unloading or reloading} \end{cases} \qquad (22)$$

The damage function ϕ serves to determine the damage parameter in terms of the state of deformation through Eq. (20). The choice of ϕ is arbitrary subject to Eq. (21) and $\phi(1) = 0$ with η satisfying $0 < \eta \leq 1$. Ogden & Roxburgh [1999] choose ϕ to be such that

$$-\phi'(\eta) = m \times erf^{-1}\left(r(\eta-1)\right) + W_\mathrm{m} \qquad (23)$$

where m and r are positive material parameters and erf-1 ( ) is the inverse of error function. By substituting Eq. (23) into Eq. (20) and after some algebra the expression

$$\eta = 1 - \frac{1}{r} erf\left(\frac{1}{m}\left(W_\mathrm{m} - W_0(\mathbf{F})\right)\right) \qquad (24)$$

for η is obtained. Because m and r were defined to be positive and considering Eq. (21), the minimum value η_m of η may be obtained from Eq. (24)

$$\eta_\mathrm{m} = 1 - \frac{1}{r} erf\left(\frac{W_\mathrm{m}}{m}\right) \qquad (25)$$

For the purpose of finite element calculation, the pseudo-elastic model is combined with Gao's hyper-elastic material model (W_0).

3.4 A specific model to represent the Mullins effect with residual strain

We propose a specific form of the pseudo-elastic energy function to represent cyclic loading for incompressible, isotropic material with stress softening and residual strain (Fig.2). Similar to ideal stress-softening (when A′ returns to A and C returns to B in Fig.2) treated in the previous paragraph, the essence of the pseudo-elasticity theory is that material behaviour in the primary loading path is described by an elastic strain energy function $W_0(\mathbf{F})$, and in unloading, reloading or secondary unloading paths by a different strain energy function. An extra term is added to describe permanent deformation. The pseudo-elastic energy function has the following form

$$W(\mathbf{F},\eta)=\eta W_0(\mathbf{F})+f(\eta)W_r(\mathbf{F},\mathbf{F}_m)+\phi(\eta) \tag{26}$$

$W_r(\mathbf{F}, \mathbf{F}_m)$ is the strain energy related to the permanent deformation. So, the second term in the right hand of this equation is related to the phenomenon of residual strains, which depend on the strain history. $\phi(\eta)$ is referred to as a dissipation function.

From the point of initiation of unloading and beyond, the damage variable η is active. It is still taken to be dependent on the deformation gradient and following Ogden and Roxburgh [1999] this dependence can be expressed as

$$\frac{\partial W(\mathbf{F},\eta)}{\partial \eta}=W_0(\mathbf{F})+f'(\eta)W_r(\mathbf{F},\mathbf{F}_m)+\phi'(\eta)=0 \tag{27}$$

The second Piola-Kirchhoff stress is then given by

$$\boldsymbol{\tau}=2\frac{\partial W(\mathbf{F},\eta)}{\partial \mathbf{C}}=2\eta\frac{\partial W_0(\mathbf{F})}{\partial \mathbf{C}}+2f(\eta)\frac{\partial W_r(\mathbf{F},\mathbf{F}_m)}{\partial \mathbf{C}}=\eta\boldsymbol{\tau}_0+f(\eta)\boldsymbol{\tau}_r \tag{28}$$

The first term on the right hand of this equation is main effect of stress softening, therefore it is clear that we should have $0<\eta\leq1$ on the unloading path and associate unloading with decreasing η. Then, $\boldsymbol{\tau}_r$ is related to the residual stress in the original configuration. The residual strain depends nonlinearly on the maximum value of strain during the previous loading history and does not change with current state of deformation $\mathbf{F}$ or $\mathbf{C}$. Obviously, the residual stress has a similar character. Therefore

$$\boldsymbol{\tau}_r=2\frac{\partial W_r(\mathbf{F},\mathbf{F}_m)}{\partial \mathbf{C}}=\boldsymbol{\tau}_r(\mathbf{C}_m) \tag{29}$$

If the maximum value of strain is positive (tensile), the corresponding residual stress will be negative, and *vice versa*. For convenience, here we use $W_r(\mathbf{C},\mathbf{C}_m)$ and define

$$W_r(\mathbf{C},\mathbf{C}_m)=-\sum_{i=1,3}\left(K_1*(C_{iim}-1)/\sqrt{ABS(C_{iim}-1)}*C_{ii}\right) \tag{30}$$

In which K_1 is a material parameter and C_{iim} are components of the Right Cauchy-Green stretch tensor at state of maximum strain during the previous loading history. Then τ_r becomes

$$\boldsymbol{\tau}_r = 2 \begin{pmatrix} -K_1 * (C_{11m} - 1)/\sqrt{ABS(C_{11m} - 1)} \\ -K_1 * (C_{22m} - 1)/\sqrt{ABS(C_{22m} - 1)} \\ -K_1 * (C_{33m} - 1)/\sqrt{ABS(C_{33m} - 1)} \\ 0 \\ 0 \\ 0 \end{pmatrix} \tag{31}$$

When unloading initiates from the loading path of simple tension the value of C_{11m} is larger than 1 and C_{22m} as well as C_{33m} are smaller than 1. Based on Eq. (31) residual stress τ_{11} is negative and τ_{22} as well as τ_{33} are positive. These results are consistent with the physical phenomenon of simple tension with permanent deformation.

Eq. (28) shows that function $f(\eta)$ leads to a residual stress separate from the total stress. To Simplify the separation, we assume $f(\eta)$ to be directly proportional to η and takes the form,

$$f(\eta) = \frac{1 - \eta}{1 - \eta_m} \tag{32}$$

This definition ensures $f(1) \equiv 0$ on the loading path, in which $\eta = 1$, and $f(\eta_m) \equiv 1$ when the strain returns to the origin. The damage parameter η can be defined in terms of the deformation gradient. Considering that η should satisfy $0 < \eta \le 1$ and decreases when unloading evolves, η is defined as

$$\eta = \begin{cases} 1 & \text{Primary loading} \\ 1 - \dfrac{1}{r} erf\left(\dfrac{W_m - W_0}{mW_m}\right) & \text{Unloading} \\ \eta_{mr} + (1 - \eta_{mr}) erf\left(\dfrac{1}{m_1}\left(\dfrac{W_0 - W_{mr}}{W_m}\right)^{r_1}\right) & \text{Reloading} \\ \eta_{mu}\left(1 - \dfrac{1}{r} erf\left(\dfrac{W_{mu} - W_0}{mW_m}\right)\right) & \text{Secondary unloading} \end{cases} \tag{33}$$

In which W_{mr} and W_{mu} are the values of strain energy at starting reloading and second unloading point, respectively. The second Piola-Kirchhoff stress can be calculated from Eq. (28) and the incremental stress-strain relation can be derived as

$$\mathbf{D} = 4\eta \frac{\partial^2 W_0}{\partial \mathbf{C}^2} + 4 \frac{\partial W_0}{\partial \mathbf{C}} \bullet \left(\frac{\partial \eta}{\partial \mathbf{C}}\right)^T + f'(\eta) \frac{\partial W_r}{\partial \mathbf{C}} \bullet \left(\frac{\partial \eta}{\partial \mathbf{C}}\right)^T \tag{34}$$

The elastic strain energy function W_0 in the specific model is presented by Gao's model for the numerical analysis in this paper.

4   Numerical analysis and applications

The computational modelling should be capable of predicting the mechanical behaviour of any type of strain. To fulfil this goal, we examine certain simple and more complicated tests under different loading conditions to evaluate whether the proposed models possess the significant features of hyperelastic materials. The material parameters are estimated by inverse technique based on experimental data throughout this study [Hendriks, 1991].

4.1   Numerical results based on Gao's constitutive model

Compression test are first used to evaluate Gao's model. An extra simple tension test as proof will also be presented in the following paragraph. The specimen used for a tension and compression test (Pozivilova, 2003) was a cylinder from soft rubber with a diameter of 11,5mm. The initial marked length for tension was 200mm and for compression was 10,15mm, respectively.

Tension test data are used for estimating material parameters, in which one solid element represents a tension specimen and results give a=0,2625; n=1,05 in Eq. (1). To simulate compression, the requirement of uniaxial stress condition in a compression test is not yet satisfied. Since the cylindrical specimen for compression is axisymmetric and symmetric to the plane dividing the cylinder (in length) into two equal parts, an axisymmetric analysis of a half cylinder was carried out. The mesh is given in Fig. 3a. Adequate boundary conditions were prescribed to agree with the experimental conditions. An identical displacement was prescribed at all nodes in the upper cross-section of the cylinder. The values of parameters estimated from tension test data are used. The distribution of the Von Mises stress on deformed specimen for compression to 40% of its original length is given in Fig. 3b. The loading force can be calculated as a sum of reactions in all nodes belonging to the bottom of the pressure head. Fig. 3c illustrates the comparison between the numerical results and experimental data. We can see that Gao's model is suitable for describing the mechanical response in the compression regime (stretch smaller than 1).

4.2   Numerical results based on CDM model

The simple tension test and a pure shear test, which were carried out by Chagnon [2004] are employed to assess the CDM model and the pseudo-elastic model. The uniaxial tensile
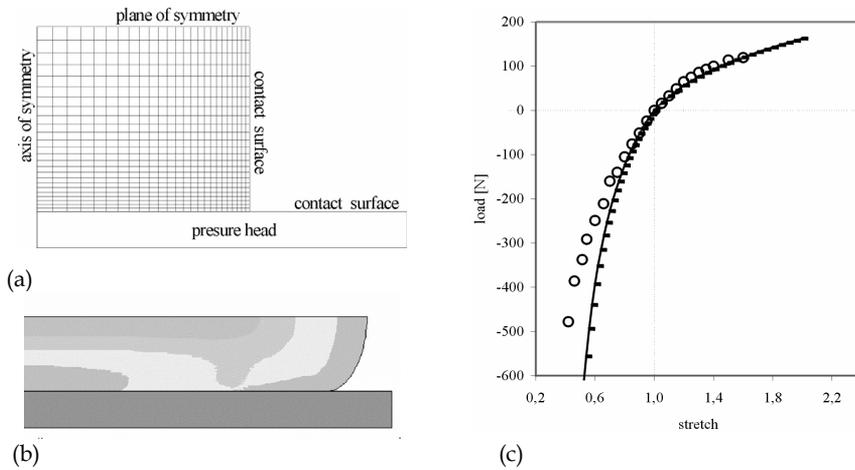
120

Figure 3. (a) FEM model of a quarter of the cylindrical specimen. (b) The stress distribution on the deformed mesh. (c) Comparison between numerical results and experimental data of the simple tension and compression: (∘ ∘ ∘) experimental data and (---) numerical results

tests were conducted on flat coupon specimens and the simple shear specimens are four blocks pieces and the simple shear experimental data are transformed into pure shear data in order to simplify the analysis (Charlton and Yang 1994). One solid element is used for the numerical calculation.

Since four material parameters (two from Gao's model and two from CDM) influence both the loading path and the unloading or reloading paths for the CDM model, the estimation of model parameters has to be manually assisted. The values of material parameters are given as $a = 0,0004$; $n = 2,5$; $d_\infty = 0,8$ and $\beta = 1,8$. The comparisons between experimental data and numerical results are illustrated in Fig. 4. From a quantitative point of view, the CDM model is not capable of reproducing all curves precisely, especially, the unloading or reloading curves. But, this approach still reveals the fundamental phenomenon of Mullins effect and predicts the behaviour involving stress softening up to large deformations. Furthermore, numerical calculations with the present approach perform well and converge rapidly.

4.3   Numerical results based on the pseudo-elastic model

In the pseudo-elastic model only two material parameters a and n from Gao's elastic model influence the loading path of the tension test. The other two parameters can be estimated from the unloading or reloading paths. These parameters can be checked with pure shear

data. The estimated values of the parameters are given as a= 0,012; n = 1,75; r= 1,45 and m=2,4. The numerical results for the tension and pure shear test were compared with experimental data in Fig. 5, respectively. Fig. 5a shows that the maximum strain in this example reaches 500% and unloading starts at a different strain level. The results in Fig. 5a are in good agreement with experiments of cyclic simple tension test even at large deformation level. The results give extra support to the use of the Gao's model. Fig. 5b illustrates that correspondence between the numerical results and experimental data for the pure shear deformation is good up to a certain amount of strain (over 300%). From the

Figure 4. Comparison between numerical results of CDM model and experimental data: (a) for cyclic tension test; (b) for cyclic pure shear test: (■) numerical results and (○) experimental data
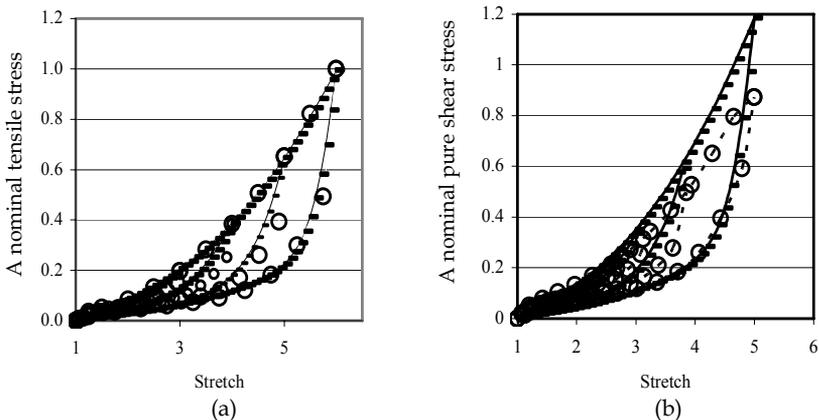

Figure 5. Comparison of numerical results of pseudo-elastic model and experimental data for cyclic tension and pure shear test: (a) simple tension and (b) pure shear: (■) numerical results and (○) experimental data

122

engineering point of view, the pseudo-elastic model combined with Gao's elastic law is capable of satisfactorily predicting the material behaviour including stress softening. Furthermore, the same material parameters are valid for different loading modes (tension and shear) applied to the specimens from the same material.

4.4   Numerical results based on the model with permanent deformation

Experiments including stress-softening and residual strain accumulation in particle-reinforced rubber [Dorfmann and Ogden 2004] are used to evaluate the model from paragraph 3.4. In the numerical calculation, primary loading is fully determined by the strain energy in Eq. (1). The model parameters a and n are estimated based on data of primary loading; K_1 is obtained by extending the unloading path until the strain returns to zero, where Eqs. (29) and (33) are activated; then, r and m may be determined based on the unloading data; and finally, the reloading data set determines the parameters r_1 and m_1. These values are summarized as follows: $a = 0{,}0457$; $n = 1{,}72$; $r = 3{,}2$; $m = 0{,}38$; $K_1 = 0{,}013$; $r_1 = 0{,}35$ and $m_1 = 1{,}2$. A comparison between numerical simulation and experimental data with 20 phr (by volume) of Carbon Black filler with maximum stretch $\lambda = 3{,}0$ is shown in Fig. 6. The numerical results are in good agreement with the experimental data. Fig. 7 illustrates the whole evolution of the cyclic loading process with maximum stretch $\lambda = 1{,}5$, $\lambda = 2{,}0$ and $\lambda = 2{,}5$. The values of all parameters used in this simulation were the same as the values used in Fig. 5, because the specimens used in the two different experiments were made of the same material.
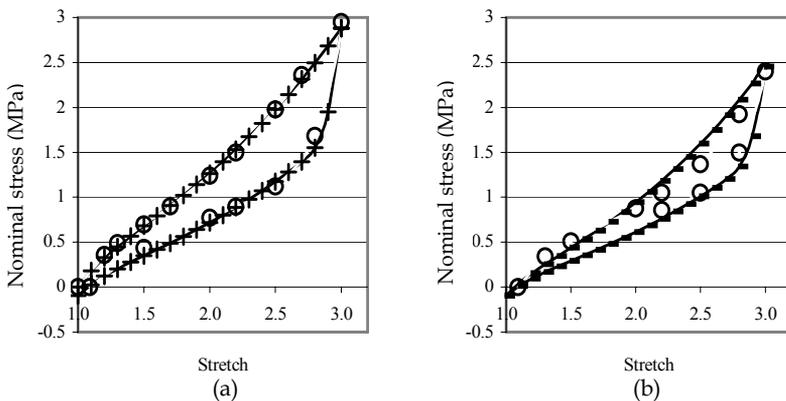

Figure 6. Comparison of nominal stress-stretch curves between numerical simulation and experimental data of uniaxial tension under cyclic loading: (a) primary loading and unloading, (b) reloading and secondary unloading. (■) experimental data, (○) numerical results
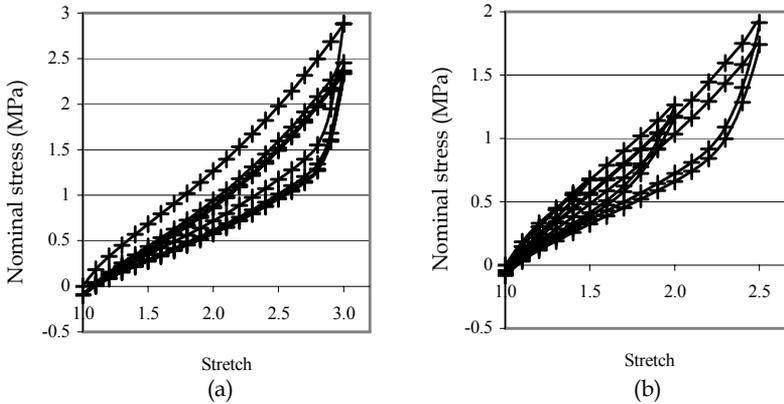
Figure 7. Nominal stress-stretch curves uniaxial tension under cyclic loading with maximum stretch λ = 3,0 in (a) and λ = 1,5, λ = 2,0 and λ = 2,5 in (b)

4.5   Application of stress-softening models

4.5.1 Shear experiment

Numerical simulations of shear-blocks, which were employed by Van den Bogert [1991] and Septanika [1998], have been carried out. The shear-blocks contain four rubber blocks and four steel members as shown in Fig. 8. The dimensions of a single rubber block are: length L=20mm, height b=10mm and thickness h=20mm. A rigid connection with the steel members is established at the upper and lower face of the rubber samples during the vulcanisation process. To create shear deformations in the rubber block a horizontal displacement is imposed in the middle steel members with a speed of approximately 100mm/minute. During the shear tests the tensile force F_t and horizontal displacement u of the middle steel member are measured. In order to compare finite element analysis with experiment, one half of a rubber specimen is modelled. The bottom plane is fixed in three directions and the top plane is allowed to displace rigidly in horizontal and vertical directions. The force F_x is applied at point P as shown in Fig. 9. So that, the relation between force F_x and horizontal displacement u_p in numerical simulation can be compared to a relation between tensile force $F_t/4$ and displacement u in the experiment since F_x is the force applied to one half of a rubber specimen and F_t is the force applied to two rubber blocks. Fig. 9. gives the typical deformation of shear-block.
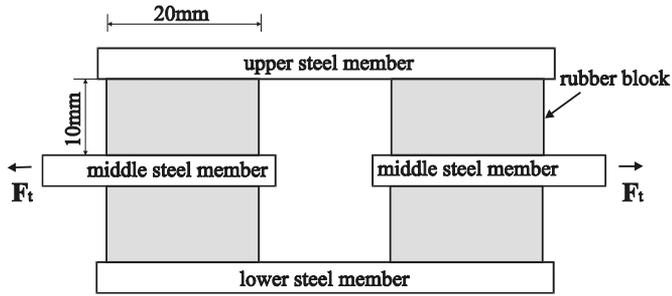
124

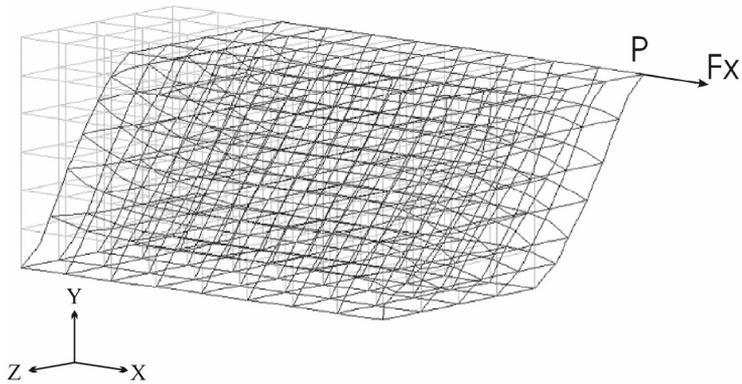*Figure 8. Construction of the specimen used in shear tests*

Figure 9. Mesh for the block-shear test: (——) undeformed and (---) deformed

a. Numerical results based on the CDM model

The combination of Gao's elastic law and the CDM model is employed and two loading cycles are considered in this simulation. The model parameters estimated based on experimental data of the first cycle of the loading path and unloading path are a=0,188; n=1,35; d_∞=0,5 and β=2,2. The identification results of the first cycle and the numerical simulation of the second cycle are compared with experimental data as shown in Fig. 10a It is difficult to choose d_∞ and β in order to separate the unloading path from the loading curve. Moreover, the values of d_∞ and β may only vary in a small range in this calculation, otherwise, divergence occurs.

b. Numerical results based on the pseudo-elastic model

The numerical results of the combination of the pseudo-elastic model and Gao's elastic law are different from the results of the CDM model. Two loading cycles are considered in this

simulation. The inverse technique is used to estimate the model parameters as we discussed in former paragraph. The model parameters are estimated based on the data of the first cycle of the loading path and unloading paths, respectively. The values of the parameters are given as: $a = 0{,}238$; $n = 1{,}05$; $r = 2{,}85$; $m = 0{,}35$. The identification results of the first cycle and the numerical simulation of the second cycle are compared with experimental data as shown in Fig. 10b. These results verify the capability of the combination of the pseudo-elastic model and Gao's elastic law in describing large shear deformation of rubber materials under cyclic loading.

4.5.2 A strip with a hole subjected to tension loading

We now investigate the model response for an inhomogeneous 3D problem. To this end, we consider the deformation of a $20{\times}20{\times}2$ mm³ strip with a circular hole with a diameter of 10mm (Fig. 11a) and employ eight-node solid elements in the calculation. The prescribed boundary conditions in the loading direction at one side allow free contraction of the specimen. The specimen is loaded at the opposite side by means of displacement controlled cyclic deformations. Bottom and top of the strip are not constrained. Two cycles with a certain displacement, at which unloading starts, are recorded. There is no wrinkling in the transverse direction during the cyclic loading.
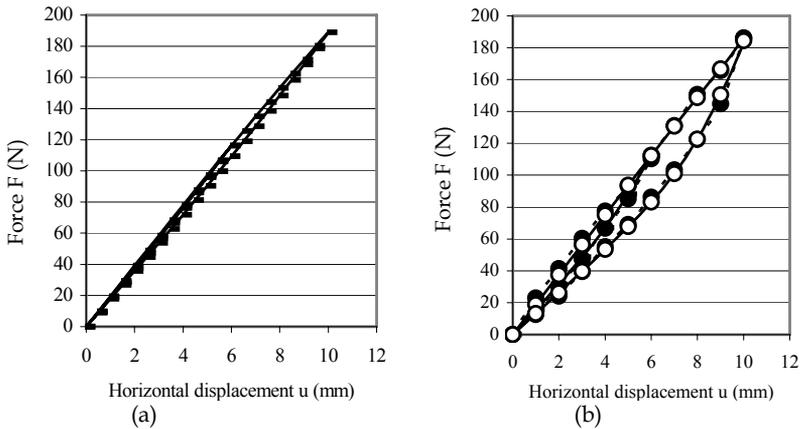

Figure 10. (a) Numerical results from CDM model (b) Comparison between numerical simulations from the pseudo-elastic model and experimental data for cyclic shear-loading test: (■) numerical results and (○) experimental data

Fig. 11b gives the deformed mesh at 200% deformation. Observe that the inhomogeneous deformation is concentrated in the neighbourhood of the hole. Stress distribution is inhomogeneous in the neighbourhood of the hole too and remains approximately homogeneous at a small distance away from the hole, which coincides with common knowledge. The maximum stress occurs at top and bottom points of the circular hole.

a. Numerical results based on the CDM model

Fig. 12a illustrates the numerical curve of the loading force against displacement based on the CDM model with parameters a=1,0, n=1,5, d_∞=0,5 and β=2,0. Two cycles of loading and unloading with respective maximum deformations of 100% and 200% are recorded. Stresses decrease after unloading takes place and the difference of maximum stress on loading and unloading path at the same deformation level (100%) reaches approximately 14% in this case.

b. Numerical results based on the pseudo-elastic model

The numerical simulation of this problem activates all model parameters involved in pseudo-elastic model and Gao's elastic law. Fig. 12b illustrates the numerical curve of the loading force against the displacement based on the pseudo-elastic model with model parameters a=1,0, n=1,5, r=2,0 and m=2,0. Stresses decrease after unloading takes place and the difference of maximum stress on loading and unloading path at the same deformation level (100%) reaches almost 50% in this case. The curves in Fig. 12b show that the cyclic process is adequately predicted. However, we should also indicate that at the onset of unloading, the step size in the computation must be taken relatively small. Otherwise, divergence will occur during the calculation process.
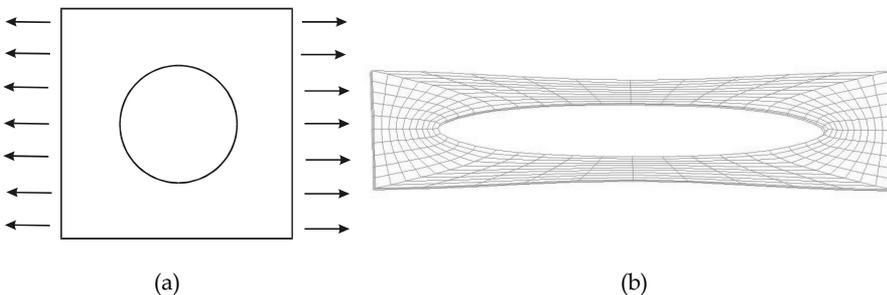

(a)　　　　　　　　　　　　　　　　　　(b)

Figure 11. (a) Specimen of a strip with a hole; (b) 200% deformed mesh of rubber strip with a hole
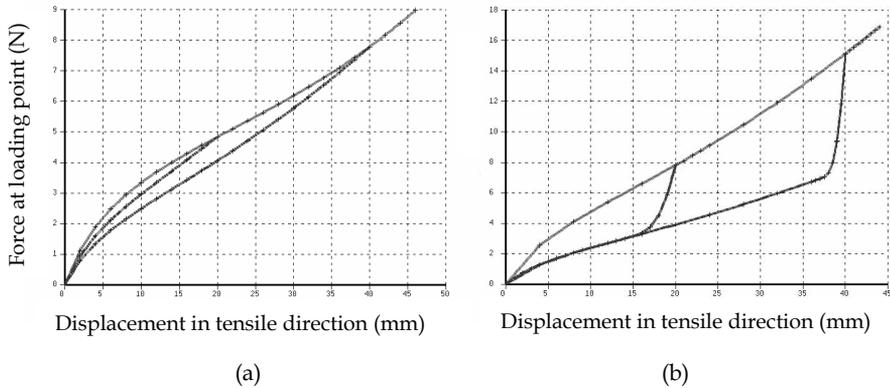
Figure 12. Load-displacement curves of Rubber strip with a hole (a) based on CDM (b) Based on pseudo-elastic model

5 Discussion

As the above results illustrate, the CDM model and the pseudo-elastic model have their own limitations and advantages. In the CDM model it is assumed that Mullins-type damage accumulation occurs only in the first cycle of a strain-controlled loading process and further strain cycles below the maximum effective strain energy give no damage contribution. So, both the parameters of the elastic law and the parameters of the CDM model influence the stress-strain relationship of the loading path and unloading or reloading paths. Since these contributions are mixed the validation of the model is more complicated.

The pseudo-elastic model phenomenologically describes the fact that the stress and strain are uniquely related in each branch of a specific cyclic process. Because the stress-softening function is activated only on the unloading or reloading paths, the pseudo-elastic model significantly simplifies the identification of model parameters. The elastic law can be determined by means of the loading path and the parameters of the pseudo-elastic model follow from unloading or reloading paths.

From an engineering point of view, the pseudo-elastic model combined with Gao's elastic law is capable of satisfactorily predicting the material behaviour including stress softening. The same material parameters are valid for different loading situations applied to the specimens from the same material. This property is crucial for the general use of the material model. Moreover, this combination is easily applied to engineering applications because of a relatively simple identification of model parameters.

6   Conclusions

The present work demonstrates the ability of Gao's elastic law to describe mechanical behaviour of rubber-like materials in the range of technical applications. Discussion on Drucker's stability postulate and results of numerical calculations show that Gao's model is stable in large strain finite element analyses.

The present work demonstrates that both the CDM model and Ogden & Roxburgh's pseudo-elastic model combined with Gao's elastic law are capable of simulating the typical Mullins effect for rubber-like materials. Since the extent of damage sustained by the material is controlled by the maximum energy state, these models are readily applicable to three-dimensional analyses.

Combination of the pseudo-elastic concept and Gao's model was used to construct a specific model for the description of Mullins effect with permanent deformation. The new damage variable totally involves five parameters and could be estimated separately according to the different branches of the evolution curves. The parameter estimation based on a specific cyclic loading case are successfully applied to different specimens with a different cyclic loading in order to validate the model.

Literature

Beatty M.F. Krishnaswamy, S. (2000) A theory of stress softening in incompressible isotropic elastic materials. *Journal of the Mechanics and Physics of Solids* 48, 1931–1965.

Besdo D., Ihlemann J. (2003) A phonological constitutive model for rubberlike materials and its numerical applications. *International Journal of plasticity* 19, 1019-1036.

Boyce M. C., Arruda E. M. (2000) Constitutive models of rubber elasticity: a review. *Rubber Chemistry Technology* 73, 504-523.

Bueche F. (1961) Mullins effect and rubber-filler interaction. *Journal of applied polymer Science* 5, 271-281.

Chagnon G., Verron E., Gornet L., Marckmann G., Charrier P. (2004) On the relevance of Continuum Damage Mechanics as applied to the Mullins effect in elastomers. *Journal of the Mechanics and Physics of Solids* 52 (7), 1627-1650.

Charlton D. J., Yang J. (1994) A review of methods to characterize rubber elastic behaviour for use in finite element analysis. *Rubber Chemistry and technology* 67, 481-503.

Dorfmann A., Ogden R.W. (2004) A constitutive model for the Mullins effect with permanent set in particle-reinforced rubber. *International Journal of Solids and Structures* 41, 1855-1878.

Drozdov A.D., Dorfmann A. (2001) Stress-strain relations in finite viscoelastoplasticity of rigid-rod networks: applications to the Mullins effect, *Continuum Mechanics and Thermodynamics* 13, 183-205.

Flory P.J., Rehner Jr. J. (1943) Statistical mechanics of cross-linked polymer networks: I. Rubberlike elasticity. *Journal of Chemical Physics* 11, 512-520.

Gao Y.C. (1997) Large deformation field near a crack tip in a rubber-like material. *Theoretical and Applied Fracture Mechanics* 26, 155-162.

Gent A. (1996) A new constitutive relation for rubber. *Rubber Chemistry and Technology Journal* 69, 59-61.

Govindjee S., Simó J.C. (1992a) Trasition from micro-mechanics to computationally efficient phenomenology: carbon black filled rubbers incorporating Mullins' effect. *Journal of the Mechanics and Physics of Solids* 40, 213-233.

Govindjee S., Simó J.C. (1992b) Mullins' effect and the strain amplitude dependence of the storage modulus. *International Journal of Solids and Structures* 29, 1737-1751.

Guo Z. (2006) *Computational modeling of rubber-like materials under monotonic and cyclic loading*. Ph.D. thesis, Delft University of Technology, the Netherlands.

Gurtin M.E., Francis E.C. (1981) Simple rate-independent model for damage. *Journal of Spacecraft* 18, 285-286.

Harwood J.A.C., Mullins L., Payne A.R. (1967) Stress softening in rubbers – A review. *Journal of the Institution of the Rubber Industry* 1, 17-27.

Hendriks M.A.N. (1991) *Identification of the mechanical behaviour of solid material.* Ph.D. thesis, Eindhoven University of Technology, the Netherlands.

James H.M., Guth E. (1943) Theory of elastic properties of rubber. *Rubber Chemistry and Technology* 11, 455-481.

Johnson M.A., Beatty M.F. (1993) A constitutive equation for the Mullins effect in stress controlled uniaxial extension experiments. *Continuum Mechanics and Thermodynamics* 5, 301-318.

Johnson, A.R., Quigley, G.J., Mead, J.L., (1994) Large strain viscoelastic constitutive models for rubber, part I: formulations. Rubber Chemistry and Technology 67, 904-917.

Kachanov L. M. (1986) *Introduction to continuum damage mechanics*. Martinus Nijhoff Publishers, Dordrecht, The Netherlands.

Knowles J.K., Sternberg Eli. (1973) An asymptotic finite deformation analysis of the elasto-static field near the tip of a crack. *Journal of Elasticity* 3, 67-107.

Kuhn W., Grun F. (1942) Beziehungen zwischen elastischen Konstanten und Dehnungsdoppelbrechung hochelastischer stoffe. Kolloid-Z 101, 248-271.

Lemaitre J., Chaboche J.L. (1990) *Mechanics of solid materials*, Cambridge University Press, Cambridge.

Lion A. (1996) A constitutive model for carbon black filled rubber: experimental investigations and mathematical representation. *Continuum Mechanics and Thermodynamics* 8, 153-169.

Miehe C. (1995) Discontinuous and continuous damage evolution in Ogden-type large-strain elastic materials. *European Journal of Mechanics. A/Solids* 14, 697-720.

Miehe C., Göktepe S., Lulei F. (2004) A micro-macro approach to rubber-like materials—Part I: the non-affine micro-sphere model of rubber elasticity. *Journal of the Mechanics and Physics of Solids* 52, 2617-2660.

Miehe C., Keck J. (2000) Superimposed finite elastic–viscoelastic–plastoelastic stress response with damage in filled rubbery polymers. Experiments, modelling and algorithmic implementation. *Journal of the Mechanics and Physics of Solids* 48, 323-365.

Mooney M.A. (1940) A theory of large elastic deformation. *Journal of Applied Physics* 11, 582-592.

Mullins L., Tobin N. R. (1957) Theoretical model for the elastic behaviour of filler-reinforced vulcanized rubbers. *Rubber Chemistry Technology* 30, 555-571.

Mullins L. (1947) Effect of stretching on the properties of rubber. *Journal of rubber research* 16, 275-289.

Ogden R. W., Roxburgh D.G. (1999) A pseudo-elastic model for the Mullins effect in filled rubber. Proceedings of Royal Society London A 455, pp. 2861-2877.

Ogden R.W. (1972a) Large deformation isotropic elasticity – on the correlation of theory and experiment for the incompressible rubber-like solids. Proceedings of Royal Society London A 326, pp. 565-584.

Ogden R.W. (1972b) Large deformation isotropic elasticity – on the correlation of theory and experiment for the compressible rubber-like solids. Proceedings of Royal Society London A 328, pp. 567-583.

Pozivilova, A. (2003) *Constitutive modelling of hyperelastic materials using the logarithmic description*. PhD thesis, the Czech Technical University in Prague.

Qi H.J., Boyce M. C. (2004) Constitutive model for stretch-induced softening of the stress-stretch behaviour of elastomeric matereials. *Journal of the Mechanics and Physics of Solids* 52, 2187-2205.

Rivlin R. S. (1948a) Large elastic deformations of isotropic materials I, Fundamental concepts. *Philosophical Transations of the Royal Society of London* A 240, pp. 459-490.

Rivlin R. S. (1948b) Large elastic deformations of isotropic materials IV, Further developments of the general theory. *Philosophical Transactions of the Royal Society of London* A 241, pp. 379-397.

Septanika E G. (1998) *A time-dependent constitutive model for filled and vulcanised rubbers*. PhD thesis. Delft University of Technology, the Netherlands.

Simo J. C. (1987) On a fully three dimensional finite strain viscoelastic damage model: Formalation and computation aspects. *Computer Method in Applied Mechanics and Engineering* 60, 153-173.

Treloar L.R.G. (1946) The elasticity of a network of long-chain molecules. *Transactions of Faraday Society* 42, 83-94.

Treloar L.R.G. (1944) Stress-strain dat for vulcanised rubber under various types of deformation. *Transactions of the Faraday Society* 40, 59-70.

van den Bogert P.A.J. (1991) *Computational modelling of rubberlike materials*. Ph.D. thesis, Delft University of Technology, the Netherlands.

Wang M.C., Guth E. (1952) Statistical theory of networks of non-Gaussian flexible chains. *Journal of Chemical Physics* 20, 1144-1157.

Wu P.D., van der Giessen E. (1993) On improved 3-D non-gaussian network models for rubber elasticity and their applications to orientation hardening in glassy polymers. *Journal of the Mechanics and Physics of Solids* 41, 427-456.

Yeoh O.H. (1993) Some forms of strain energy function for rubber. *Rubber Chemistry and Technology* 66, 754-771.

Zhong A. (2005) Discussion "A constitutive model for the Mullins effect with permanent set in particle-reinforced rubber" by A. Dorfmann and R.W. Ogden. *International Journal of Solids and Structures* 42, 3967-3969.